11

ESSENTIALS IN WAVELET THEORY

§11.1 GOOD WAVELET PROPERTIES

Now that we have applied wavelets to extract Impulse Response Functions (IRFs) using the Fast Wavelet Transform, we ask ourselves what features in wavelet basis functions provide the desirable characteristics in structural system identification. Of several possible approaches to the understanding of wavelets, we adopt the filter banks concepts advocated by Strang and Nguyen. If we are to be intelligent users of wvelets in our applictions, it is important that we understand the four essential properties of wavelets:

Perfect Reconstruction (PR Condition)

Orthogonality (Condition O)

Accuracy in the pth order (Condition A_p)

Stability (Condition E)

The PR condition ensures that the output reconstructs the input with a time delay, a critical property for multiresolution purposes which will be shortly elaborated. The orthogonality condition provides, first of all, lossless transform plus aliasing cancellation and preserves linear phase between the input and output, in addition to maintaining the level-by-level linear independence in multiresolution analysis. The condition A_p is a measure of the accuracy of the filter. Finally, the condition E is prerequisite for filter output stability. We now examine these four properties below so that we can select a most derirable wavelet for each application out of a plethora of wavelet bases.

§11.2 WHAT IS MULTIRESOLUTION?

Let us recall the approximation of a function $f(t)$ by a wavelet in a general form:

$$f(t) = \sum_{j,k} b_{jk}\, w_{jk}(t) \tag{11.1}$$

where k is the filter tap counter, j is the multiresolution level, w_{jk} the wavelet at level j correspondingto the k-th tap.

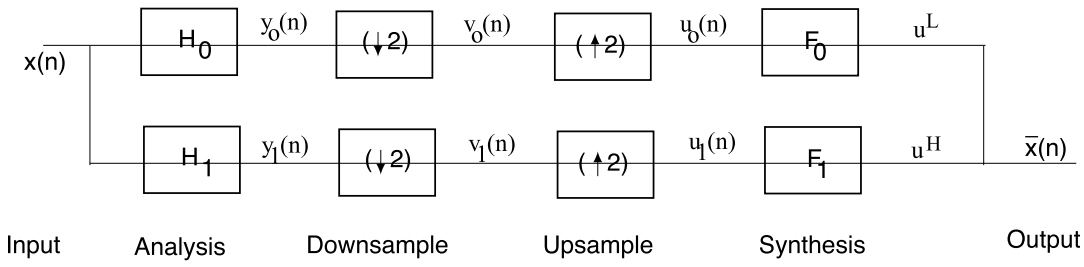

Figure 11.1 Two-Channel Filter Banks

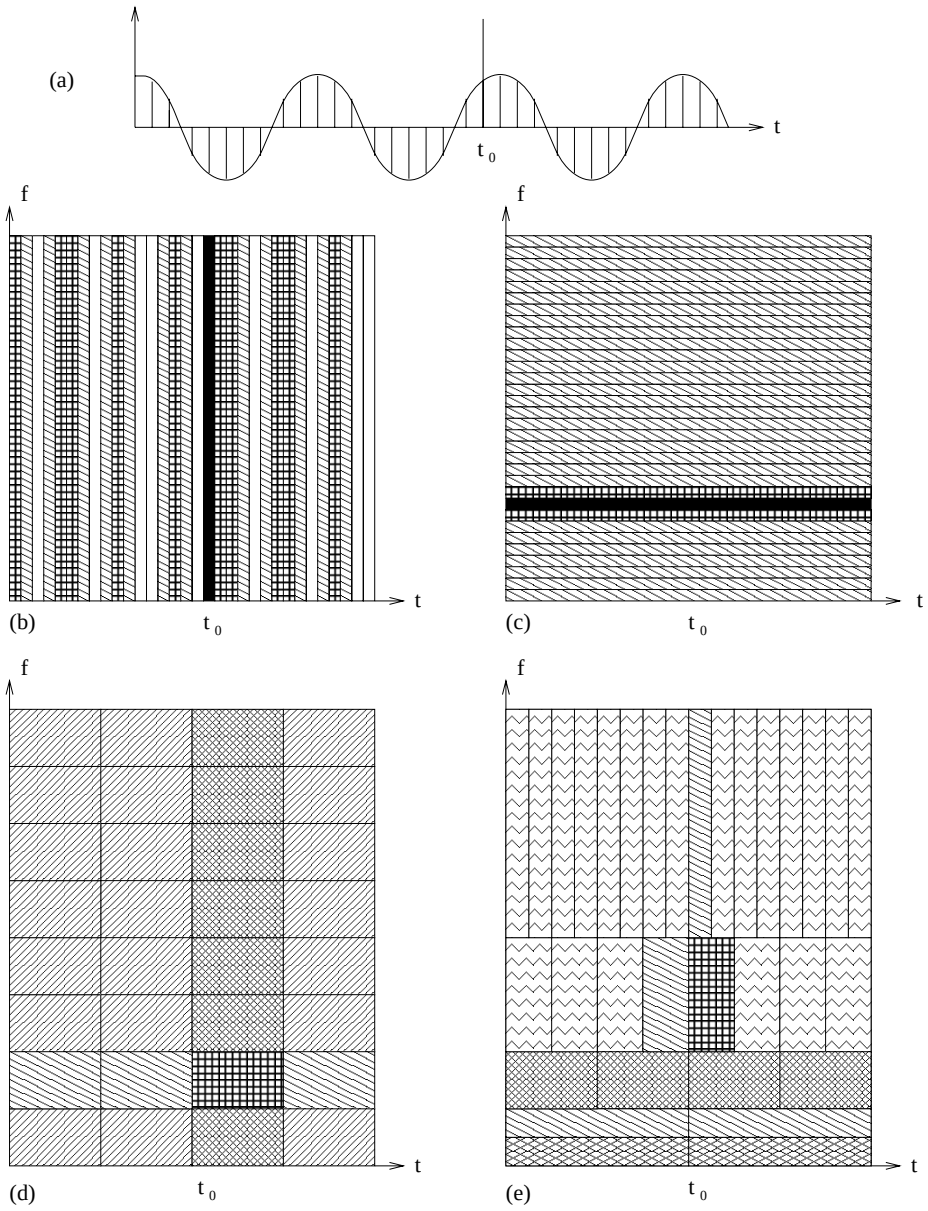

Figure4.2 Frequency/Time Tiling of a Discrete Signal. (a) Sine Signal with Discontinuity (b) Identity Transform (c) Discrete Fourier Transform (d) Short Time Fourier Transform (e) Discrete Wavelet Transform

Fourier transforms are also capable of obtaining time information about a signal if a windowing procedure is used to create a **S**hort **T**ime Fourier transform (STFT). The window is a square wave which truncates the sine or cosine function to fit a window of a particular width. Since the same window is used for all frequencies, the resolution is the same at all positions in the time-frequency plane as seen in figure test. The discrete wavelet transform (DWT), on the other hand, has a window size that varies frequency scale. This is advantageous for the analysis of signals containing both discontinuities and smooth components. Short, high frequency basis functions are needed for the discontinuities, while at the same time, long low frequency ones are needed for the smooth

components. This is exactly the type of time-frequency tiling you get from wavelet transforms. Figure 4.1 depicts this relationship by showing how the time resolution gets finer as the scale (or frequency) increases. Each basis function is represented by a tile, where the shading corresponds to the value of the expansion coefficient.

An example of this representation is provided by the analysis of a discrete sine signal (with a discontinuity) portrayed in Fig. 4.2(a)-(d). The upper two figures, (b) and (c), display the identity and discrete Fourier transform of the given signal. The first is able to isolate the location of the impulse while the second is able to isolate the frequency band of the sine signal, neither is able to do both. By using a windowing function with the Fourier transform (d) , one is now able to see both the impulse and frequency of the sine signal, but with a loss of resolution. The wavelet transform (e), on the other hand, is able to achieve better localization of the time-domain impulse with a slightly inferior frequency resolution. For a higher-frequency sine function, however, the frequency localization would be much worse when using a wavelet transform. From this example, one can see some of the trade-offs between wavelet and Fourier transforms.

An important feature of both wavelet and Fourier transforms is the orthogonality of their basis functions, which allows for a unique representation of the signal being analyzed. Orthogonality enables any function, f, to be represented by:

$$f = \sum_x < f, x > x \tag{11.2}$$

where x are the basis functions and $< f, x >$ is the inner product of f and x. Resulting from this is Parseval's theorem, which relates the energy of the original signal to that of the transformed signal:

$$|| f ||^2 = \sum_x | < f, x > |^2 \tag{11.3}$$

The relation states that the energy of the original time series is preserved in the transform coefficients. This means that the choice of the orthogonal basis you use determines whether the energy decomposition with respect to the transformed coefficients provides interesting information about the original time series.

Using equation (11.2), a function, f, can be represented by either wavelet or Fourier basis functions:

$$\begin{aligned} Wavelet: f(t) &= \sum_{J,k} < f(t), \psi(2^J t - k) > \psi(2^J t - k) \\ &= b_0 \phi(t) + \sum_{J,k} b_{2^J+k} \cdot \psi(2^J t - k) \\ Fourier: f(t) &= \sum_m < f(t), e^{-jm\omega_0 t} > e^{-jm\omega_0 t} \\ &= \sum_m a_m e^{-jm\omega_0 t} \end{aligned} \tag{11.4}$$

where ψ are the dilated and translated wavelet basis functions, ϕ is the scaling function (also a wavelet basis function), and $e^{-jm\omega_0 t}$ are the Fourier basis functions. The result of the inner product

of f with the basis functions is the transform of that signal, a, termed either the wavelet or Fourier coefficients. In order to understand the structure of the wavelet transform, we can arrange the wavelet coefficients into the following form:

$$\begin{aligned} f^{wav}(t) &= b_0\phi(t) + b_1\psi(t) \\ &+ [b_2 \;\; b_3]\begin{bmatrix} \psi(2t) \\ \psi(2t-1) \end{bmatrix} \\ &+ [b_4 \;\; b_5 \;\; b_6 \;\; b_7]\begin{bmatrix} \psi(4t) \\ \psi(4t-1) \\ \psi(4t-2) \\ \psi(4t-3) \end{bmatrix} + \\ &+ .... + b_{(2^j+k)}\psi(2^J t - k) \end{aligned} \tag{11.5}$$

Observe that the first two terms associated with the scaling function $\phi(t)$ and mother wavelet $\psi(t)$ span the entire time, e.g., $0 \le t \le 1$. The functions associated with the next two terms, viz., $\psi(2t)$ and $\psi(2t-1)$, span $0 \le t \le 1/2$ and $1/2 \le t \le 1$, respectively, and similarly for subsequent terms with each spanning smaller and smaller intervals without overlap, thus revealing the orthogonality of the local basis functions. Qualitatively speaking, the $\phi(t)$-term associated with the coefficient b_0 is an averaged value of $f(t)$ whereas the wavelet $\psi(t)$ associated with the coefficient b_1 may be viewed as a differencing operator spanning the entire range of t. Similarly, the next-level terms $[\psi(2t) \;\; \psi(2t-1)]$ associated with $[b_2 \;\; b_3]$ are again differencing operators, each spanning half of the range without overlap, and so on. Hence, each additional level added to the series picks out the details left out from the series approximation.

Unlike the Fourier basis functions, there are an infinite number of possible sets of wavelet basis functions. A wavelet is formed from a set of filter coefficients that must satisfy a given set of conditions (see the four conditions in page xx of Strang and Nguyen). Any set of filter coefficients which satisfy the given conditions can be used to create a wavelet function. The scaling function, or Father wavelet, of order N is then created from a dilation equation:

$$\phi(t) = \sum_{k=0}^{N-1} c_k \phi(2t-k) \tag{11.6}$$

where c_k are the filter coefficients. The wavelet functions can then be generated via:

$$\psi(t) = \sum_{k=0}^{N-1} (-1)^k c_k \phi(2t+k-N+1) \tag{11.7}$$

whose scaling and the wavelet functions must also satisfy certain normalization and orthogonalization constraints.

As mentioned previously, there are an infinite number of possible mother wavelets. Figure 4.3 shows four of the more common ones: the Haar wavelet (also Daubechies order 2 wavelet), the Daubechies order 4 wavelet, the Coiflet order 3 wavelet, and the Symmlet order 8 wavelet. The order indicates how smooth the wavelet is. It is apparent in Fig. 4.3, that a higher order, like the Symmlet 8 wavelet, means a smoother function, but it also means less compactness in time. The choice and order of the wavelet to be used should depend on the dominant features of the signal being analyzed. The basis functions should match the signal as closely as possible.

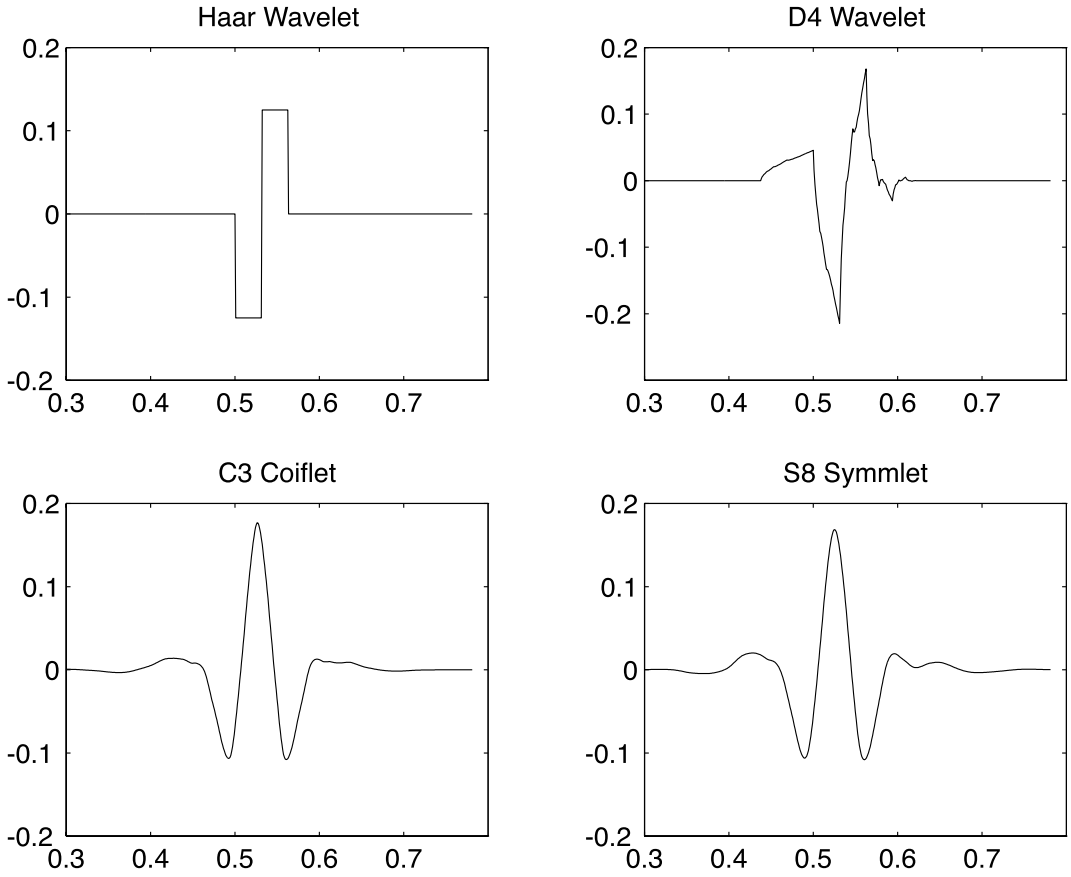

Figure 4.3 Mother Wavelet Basis Functions

To demonstrate the need for an appropriate choice of wavelet and illustrate the time/frequency nature of the wavelet transform, a Doppler signal is analyzed. Figure 4.4 shows the original signal and the wavelet transform using both the Haar and Symmlet 8 wavelets. A plot of the wavelet coefficients does not provide much insight. In order to get a better understanding, the individual frequency levels are separated out and the wavelet coefficients plotted as a function of time as shown in Figs. 4.5 and 4.6. Each frequency band spans the entire length of time, but with less and less time resolution as the frequencies get lower. On the other hand, as the frequencies getthe width of the frequency bands also decrease, meaning that more frequency resolution is provided. The magnitude of each wavelet coefficient is indicated by the height of the line representing it. In the

Symmlet 8 transform, the nature of the Doppler signal is shown, the decrease in frequency with time is apparent by the sliding of the wavelet coefficients with each increase in frequency level. The good representation is due to the similarity between the smoothness of the wavelet basis functions and the Doppler signal. On the opposite extreme, the Haar wavelet does not closely match the Doppler signal at all. This is shown in Fig. 4.6, where the decreasing frequency as a function of time is not nearly as apparent. The Haar transform does provide a good representation of how the time resolution increases with an increase in frequency. Notice that the spacing between the wavelet coefficients becomes smaller and smaller as the frequency bands increase.

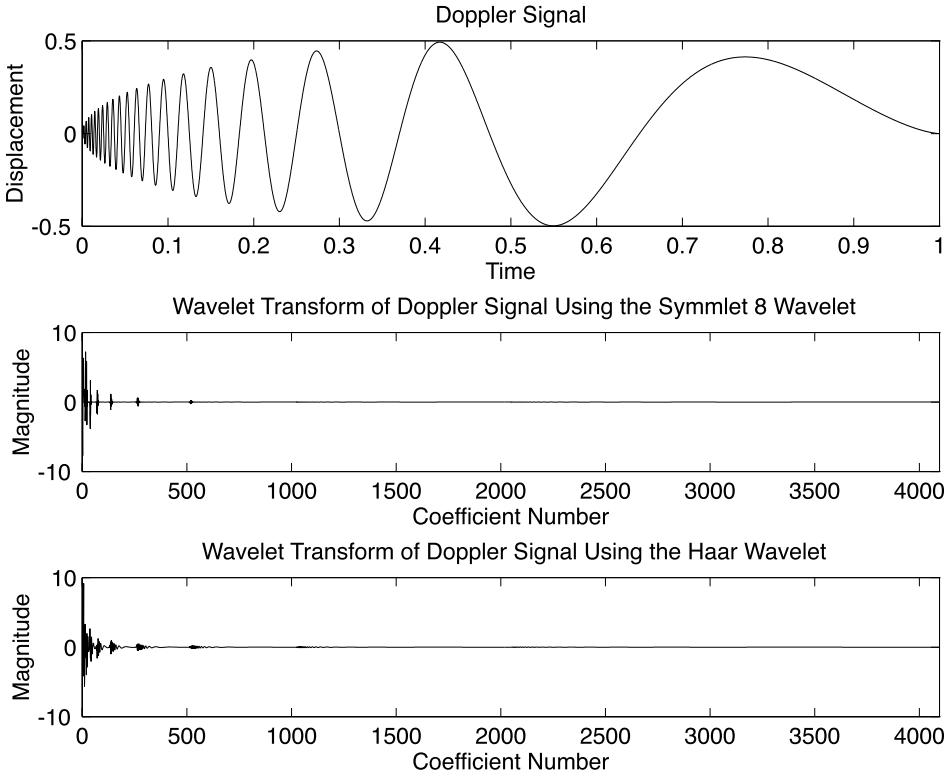

Figure 4.4 Doppler Signal and Its Wavelet Transform

We can now see clearly an important comparison between the Fourier and the wavelet expansions of $f(t)$. The Fourier expansion may be advantageous in capturing frequency characteristics in $f(t)$ whereas the wavelet expansion directly captures the temporal properties of $f(t)$. Hence, in a typical signal processing of vibration data, the discrete Fourier expansion of $f(t)$ involves first the convolution integral in the frequency domain, usually via FFT, and then an inverse FFT. In other words, in the Fourier expansion the data must be transformed from the time domain into the corresponding frequency domain and then converted again back into time domain. On the other

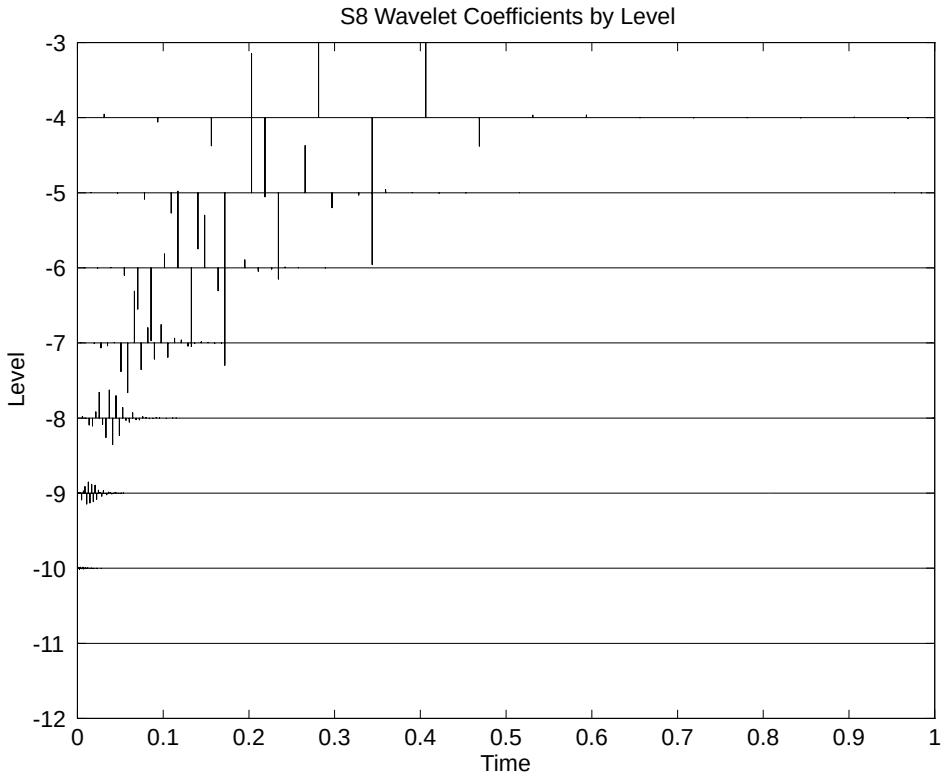

Figure 4.5 Time/Frequency Representation of Doppler Signal via S8 Wavelet Transform

hand, the wavelet expansion preserves the temporal nature of the data while also showing frequency content during both the forward and inverse wavelet transforms.

§11.3 FAST WAVELET TRANSFORM

It is generally agreed that the widespread use of the FFT has been largely due to its computational efficiency, that is, for the sampling size $n = 2^J$, the FFT has $\frac{1}{2} n \log_2 n$ multiplications. In Fast Wavelet Transform, for n data point value of $f(t)$, viz.,

$$\mathbf{f} = [\, f(0),\ f(1),\ ...,\ f(2^J - 1)]^T \tag{11.8}$$

we would like to obtain the wavelet coefficients as expressed in (11.5), the wavelet coefficients $\mathbf{b} = [b(0), b(1), ..., b(2^J - 1)]^T$ or its inverse

$$\mathbf{b} = \mathbf{A}\,\mathbf{f} \qquad \Leftarrow \ \Rightarrow \qquad \mathbf{f} = \mathbf{S}\,\mathbf{b} \tag{11.9}$$

as efficiently as possible.

To this end, let us consider the Haar function which is perhaps the simplest wavelet basis function as shown in Fig. 4.7 for $L = 2^J$, $J = 2$. The synthesis matrix $\mathbf{S}$ can be expressed as

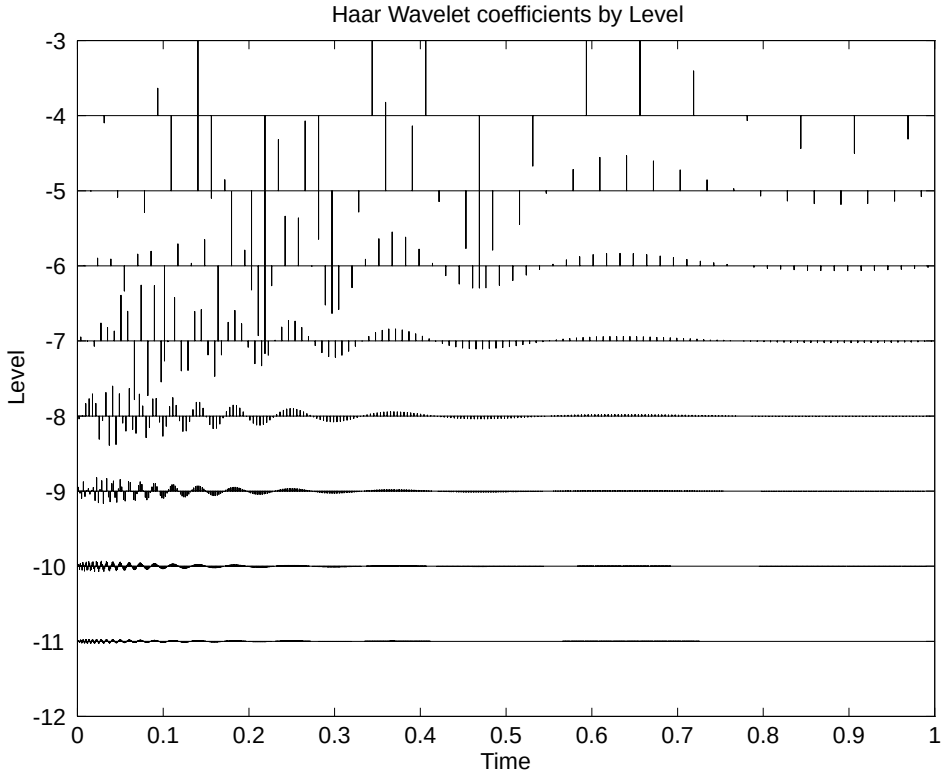

Figure 4.6 Time/Frequency Representation of Doppler Signal via Haar Wavelet Transform

$$\mathbf{S} = \begin{bmatrix} 1 & 1 & 1 & 0 \\ 1 & 1 & -1 & 0 \\ 1 & -1 & 0 & 1 \\ 1 & -1 & 0 & -1 \end{bmatrix} \tag{11.10}$$

Note that the first column in the above matrix, $\mathbf{S}(1:4,1) = [1,1,1,1]^T$, corresponds to the value of the scaling function $\{\phi(t), 1 \le t < 1\}$ as its magnitude remains for the entire time interval. The second column $\mathbf{S}(1:4,2) = [1,1,-1,-1]^T$ corresponds to the value of the wavelet function $\{w(t), 1 \le t < 1\}$ as its magnitude is 1 for $\{1 \le t < 1/2\}$ and -1 for $\{1/2 \le t < 1\}$. The third column $\mathbf{S}(1:4,3) = [1,-1,0,0]^T$ corresponds to the value of the wavelet function $\{w(2t), 1 \le t < 1/2\}$ as its magnitude is 1 for $\{1 \le t < 1/4\}$ and -1 for $\{1/4 \le t < 1/2\}$. Finally, the fourth column $\mathbf{S}(1:4,4) = [0,0,1,-1]^T$ corresponds to the value of the wavelet function $\{w(2t-1), 1/2 \le t < 1\}$ as its magnitude is 1 for $\{1/2 \le t < 3/4\}$ and -1 for $\{3/4 \le t < 1\}$.

For computational expediency as well as for incorporating the Parseval theorem, let us introduce a modified expression for $\mathbf{S}$ with a scale factor $(1/\sqrt{2})$ as:

$$\mathbf{S}_4 = \begin{bmatrix} r^2 & r^2 & r & 0 \\ r^2 & r^2 & -r & 0 \\ r^2 & -r^2 & 0 & r \\ r^2 & -r^2 & 0 & -r \end{bmatrix} \tag{11.11}$$

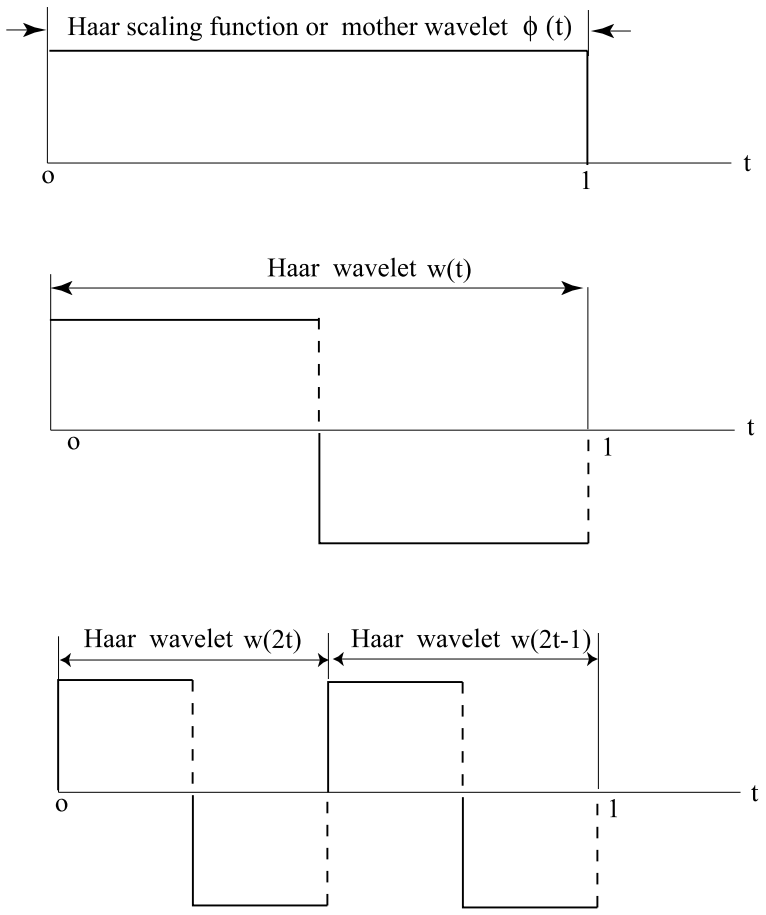

Figure 4.7 Haar Scaling Function and Wavelets

which gives unit vectors in the columns and rows since $2r^2 =$ and $4r^4 = 1$.

The key aspect that leads to the Fast Wavelet Transform is because, like in the FFT, **A** can be rearranged as a product of two matrices:

$$\mathbf{S}_4 = \begin{bmatrix} r & r & 0 & 0 \\ r & -r & 0 & 0 \\ 0 & 0 & r & r \\ 0 & 0 & r & -r \end{bmatrix} \cdot \begin{bmatrix} 1 & 0 & 0 & 0 \\ 0 & 0 & 1 & 0 \\ 0 & 1 & 0 & 0 \\ 0 & 0 & 0 & 1 \end{bmatrix} \cdot \begin{bmatrix} r & r & 0 & 0 \\ r & -r & 0 & 0 \\ 0 & 0 & 1 & 0 \\ 0 & 0 & 0 & 1 \end{bmatrix} \tag{11.12}$$

$$\Downarrow\Downarrow$$

$$\mathbf{S}_4 = \begin{bmatrix} \mathbf{S}_2 & 0 \\ 0 & \mathbf{S}_2 \end{bmatrix} \cdot \mathbf{P}_4 \cdot \begin{bmatrix} \mathbf{S}_2 & 0 \\ 0 & \mathbf{I}_2 \end{bmatrix}, \qquad \mathbf{S}_2 = \begin{bmatrix} r & r \\ r & -r \end{bmatrix}$$

For the case of 8 samples, we have

$$\mathbf{S}_8 = \begin{bmatrix} r^3 & r^3 & r^2 & 0 & r & 0 & 0 & 0 \\ r^3 & r^3 & r^2 & 0 & -r & 0 & 0 & 0 \\ r^3 & r^3 & -r^2 & 0 & 0 & r & 0 & 0 \\ r^3 & r^3 & -r^2 & 0 & 0 & -r & 0 & 0 \\ r^3 & -r^3 & 0 & r^2 & 0 & 0 & r & 0 \\ r^3 & -r^3 & 0 & r^2 & 0 & 0 & -r & 0 \\ r^3 & -r^3 & 0 & -r^2 & 0 & 0 & 0 & r \\ r^3 & -r^3 & 0 & -r^2 & 0 & 0 & 0 & -r \end{bmatrix} \tag{11.13}$$

which can be decomposed into two-matrix product:

$$\mathbf{S}_8 = \mathbf{W}_8 \cdot \begin{bmatrix} \mathbf{S}_2 & 0 \\ 0 & \mathbf{I}_6 \end{bmatrix}, \qquad \mathbf{W}_8 = \begin{bmatrix} r^2 & 0 & r^2 & 0 & r & 0 & 0 & 0 \\ r^2 & 0 & r^2 & 0 & -r & 0 & 0 & 0 \\ r^2 & 0 & -r^2 & 0 & 0 & r & 0 & 0 \\ r^2 & 0 & -r^2 & 0 & 0 & -r & 0 & 0 \\ 0 & r^2 & 0 & r^2 & 0 & 0 & r & 0 \\ 0 & r^2 & 0 & r^2 & 0 & 0 & -r & 0 \\ 0 & r^2 & 0 & -r^2 & 0 & 0 & 0 & r \\ 0 & r^2 & 0 & -r^2 & 0 & 0 & 0 & -r \end{bmatrix} \tag{11.14}$$

The matrix $\mathbf{W}_8$ can be expressed as

$$\mathbf{W}_8 = \begin{bmatrix} \mathbf{S}_4 & \\ & \mathbf{S}_4 \end{bmatrix} \cdot \mathbf{P}_8, \quad \mathbf{P}_8 = \begin{bmatrix} 1 & 0 & 0 & 0 & 0 & 0 & 0 & 0 \\ 0 & 0 & 1 & 0 & 0 & 0 & 0 & 0 \\ 0 & 0 & 0 & 0 & 1 & 0 & 0 & 0 \\ 0 & 0 & 0 & 0 & 0 & 1 & 0 & 0 \\ 0 & 1 & 0 & 0 & 0 & 0 & 0 & 0 \\ 0 & 0 & 0 & 1 & 0 & 0 & 0 & 0 \\ 0 & 0 & 0 & 0 & 0 & 0 & 1 & 0 \\ 0 & 0 & 0 & 0 & 0 & 0 & 0 & 1 \end{bmatrix} \tag{11.15}$$

Using (11.12), $\mathbf{S}_8$ can be decomposed as

$$\mathbf{S}_8 = \begin{bmatrix} \begin{bmatrix} \mathbf{S}_2 & 0 \\ 0 & \mathbf{S}_2 \end{bmatrix} \cdot \mathbf{P}_4 \cdot \begin{bmatrix} \mathbf{S}_2 & 0 \\ 0 & \mathbf{I}_2 \end{bmatrix} & \\ & \begin{bmatrix} \mathbf{S}_2 & 0 \\ 0 & \mathbf{S}_2 \end{bmatrix} \cdot \mathbf{P}_4 \cdot \begin{bmatrix} \mathbf{S}_2 & 0 \\ 0 & \mathbf{I}_2 \end{bmatrix} \end{bmatrix} \cdot \mathbf{P}_8 \cdot \begin{bmatrix} \mathbf{S}_2 & 0 \\ 0 & \mathbf{I}_6 \end{bmatrix} \tag{11.16}$$

For $\mathbf{S}_{16}$, a similar decomposition leads to

$$\mathbf{S}_{16} = \begin{bmatrix} \mathbf{S}_8 & \\ & \mathbf{S}_8 \end{bmatrix} \cdot \mathbf{P}_{16} \cdot \begin{bmatrix} \mathbf{S}_2 & 0 \\ 0 & \mathbf{I}_{14} \end{bmatrix} \tag{11.17}$$

Now, extensions to an arbitrary number of samples, $L = 2^J$ is straightforward. Finally, it should be pointed that the real utility of the above decompositions is to obtain the wavelet-transformed coefficients **b**. This can be accomplished by invoking the relation:

$$\mathbf{b} = \mathbf{A}\,\mathbf{f}, \quad \mathbf{A} = \mathbf{S}^T \tag{11.18}$$

It must be emphasized that the fast wavelet transform algorithm detailed above for the Haar wavelet is applicable to other wavelets.

§11.4 MALLAT'S PYRAMID ALGORITHM

In the preceding section we have presented the Fast Wavelet Transform in terms of linear algebra. A more appealing procedure was presented by S. Mallat in 1989 that utilizes the decomposition of the wavelet transform in terms of low pass (aeraging) filters and high pass (diferencing) filters. To illustrate Mallat's pyramid algorithm, let's reconsider the case of 8 samples. Since $\{2J = 8 \rightarrow J = 3\}$, we need three filters each for both low and high pass filters, which for the case of Haar wavelet are expressed as

Low Pass Filters:

$$\begin{aligned} L_1 &= \tfrac{1}{2}\begin{bmatrix} 1 & 1 \end{bmatrix} \\ L_2 &= \tfrac{1}{2}\begin{bmatrix} 1 & 1 & & \\ & & 1 & 1 \end{bmatrix} \\ L_3 &= \tfrac{1}{2}\begin{bmatrix} 1 & 1 & & & & & & \\ & & 1 & 1 & & & & \\ & & & & 1 & 1 & & \\ & & & & & & 1 & 1 \end{bmatrix} \end{aligned} \tag{11.19}$$

High Pass Filters:

$$\begin{aligned} H_1 &= \tfrac{1}{2}\begin{bmatrix} -1 & 1 \end{bmatrix} \\ H_2 &= \tfrac{1}{2}\begin{bmatrix} -1 & 1 & & \\ & & -1 & 1 \end{bmatrix} \\ H_3 &= \tfrac{1}{2}\begin{bmatrix} -1 & 1 & & & & & & \\ & & -1 & 1 & & & & \\ & & & & -1 & 1 & & \\ & & & & & & -1 & 1 \end{bmatrix} \end{aligned}$$

First, we group the wavelet transformed coefficient vector $\mathbf{b}$ into three transform levels:

$$\mathbf{b}^T = [\,\mathbf{a}^0, \mathbf{b}^0, \mathbf{b}^1, \mathbf{b}^2\,] = [\,[b_0], [b_1], [b_2, b_3], [b_4, b_5, b_6, b_7]\,] \tag{11.20}$$

In the pyramid algorithm, we first compute the third-level wavelet transform coefficients $\mathbf{b}^{J-1} = [b_4, b_5, b_6, b_7]^T$ via

$$\mathbf{b}^2 = H_3\,\mathbf{a}^3, \qquad \mathbf{a}^3 = \mathbf{x} \tag{11.21}$$

Second, we obtain the second-level averaging vector $\mathbf{a}^{J-1}$ via

$$\mathbf{a}^2 = \mathbf{L}_3\,\mathbf{a}^3 \tag{11.22}$$

The first-level wavelet transform coefficients $\mathbf{b}^1$ is now obtained by

$$\mathbf{b}^1 = [b_2, b_3]^T = \mathbf{H}_2\, \mathbf{a}^2 = \mathbf{H}_2\mathbf{L}_3\mathbf{x} \tag{11.23}$$

We then compute the first-level averaging coefficients $\mathbf{a}^0$ via

$$\mathbf{a}^1 = \mathbf{L}_2\, \mathbf{a}^2 = \mathbf{L}_2\, \mathbf{L}_3\, \mathbf{x} \tag{11.24}$$

The zeroth-level wavelet transform coefficient $\mathbf{b}^0$ is obtained by

$$\mathbf{b}^0 = b_1 = \mathbf{H}_1\, \mathbf{a}^1 = \mathbf{H}_1\mathbf{L}_2\mathbf{L}_3\, \mathbf{x} \tag{11.25}$$

Finally, the zeroth-level coefficient that corresponds to the scaling function is obtained by

$$\mathbf{a}^0 = b_0 = \mathbf{L}_1\mathbf{a}^1 = \mathbf{L}_1\mathbf{L}_2\mathbf{L}_3\, \mathbf{x} \tag{11.26}$$

There are wavelets whose scaling functions require more than two parameters. For example, the Daubechies D_4 wavelet scaling and wavelet functions:

$$\begin{aligned}
\phi^{D_4}(t) &= \sum_{k=0}^{3} c_k\, \phi(2t-k) \\
c_0 &= \frac{1}{4}(1+\sqrt{3}), \quad c_1 = \frac{1}{4}(3+\sqrt{3}) \\
c_2 &= \frac{1}{4}(3-\sqrt{3}), \quad c_3 = \frac{1}{4}(1-\sqrt{3}) \\
\psi^{D_4}(t) &= \sum_{k=0}^{3} h_k\, \phi(2t-k) \\
h_0 &= -c_3 = \frac{1}{4}(1-\sqrt{3}), \quad h_1 = c_2 = \frac{1}{4}(3-\sqrt{3}) \\
h_2 &= -c_1 = \frac{1}{4}(3+\sqrt{3}), \quad h_3 = c_0 = \frac{1}{4}(1+\sqrt{3})
\end{aligned} \tag{11.27}$$

The corresponding low and high pass filters are constructedd as

Low Pass Filters:

$$
\begin{aligned}
L_1 &= \tfrac{1}{2}\,[\,c_3 \quad c_2 \quad c_1 \quad c_0\,] \Rightarrow \tfrac{1}{2}\,[\,c_3 + c_1 \quad c_2 + c_0\,] \text{ (due to wrap around)} \\
L_2 &= \tfrac{1}{2}\begin{bmatrix} c_3 & c_2 & c_1 & c_0 & & \\ & & c_3 & c_2 & c_1 & c_0 \end{bmatrix} \Rightarrow \tfrac{1}{2}\begin{bmatrix} c_3 & c_2 & c_1 & c_0 \\ c_1 & c_0 & c_3 & c_2 \end{bmatrix} \text{ (wrap around)} \\
L_3 &= \tfrac{1}{2}\begin{bmatrix} c_3 & c_2 & c_1 & c_0 & & & & \\ & & c_3 & c_2 & c_1 & c_0 & & \\ & & & & c_3 & c_2 & c_1 & c_0 \\ c_1 & c_0 & & & & & c_3 & c_2 \end{bmatrix}
\end{aligned}
\tag{11.28}
$$

High Pass Filters:

$$
\begin{aligned}
H_1 &= \tfrac{1}{2}\,[\,h_3 \quad h_2 \quad h_1 \quad h_0\,] \Rightarrow \tfrac{1}{2}\,[\,h_3 + h_1 \quad h_2 + h_0\,] \text{ (due to wrap around)} \\
H_2 &= \tfrac{1}{2}\begin{bmatrix} h_3 & h_2 & h_1 & h_0 & & \\ & & h_3 & h_2 & h_1 & h_0 \end{bmatrix} \Rightarrow \tfrac{1}{2}\begin{bmatrix} h_3 & h_2 & h_1 & h_0 \\ h_1 & h_0 & h_3 & h_2 \end{bmatrix} \\
H_3 &= \tfrac{1}{2}\begin{bmatrix} h_3 & h_2 & h_1 & h_0 & & & & \\ & & h_3 & h_2 & h_1 & h_0 & & \\ & & & & h_3 & h_2 & h_1 & h_0 \\ h_1 & h_0 & & & & & h_3 & h_2 \end{bmatrix}
\end{aligned}
$$

For the Daubechies wavelet, the Mallat algorithm detailed in (11.21) - (11.26) is equally applicable. We now formalize Mallat's pyramid algorithm for a data set with 2^J samples:

Decomposition (to obtain the wavelet transform coefficients b):

Initialize $\mathbf{a}^J = \mathbf{x}$. For $j = J, (J-1), ..., 1$ compute

$$\mathbf{a}^{j-1} = \mathbf{L}_j\,\mathbf{a}^j \qquad \text{and} \qquad \mathbf{b}^{j-1} = \mathbf{H}_j\,\mathbf{a}^j \tag{11.29}$$

Eventually, after carrying out the necessary complex computations such as denoising and convolutions, one would like to reconstruct the desired signal for subsequent signal processing or future applications. The reconstruction is simply a transposition of the decomposition, which can be summarized as

Reconstruction (to obtain the enhanced signal x):

Start with $\mathbf{a}^0$ and $\mathbf{b}^0, \mathbf{b}^1, ..., \mathbf{b}^{J-1}$. For $j = 1, 2, ..., J$ compute

$$\mathbf{a}^j = \mathbf{L}_j^T\,\mathbf{a}^{j-1} + \mathbf{H}_j^T\,\mathbf{b}^{j-1}$$

$$\Downarrow$$

$$\hat{\mathbf{x}} = \mathbf{a}^J$$

where $\hat{\mathbf{x}}$ is the reconstructed signal

(11.30)

References for Wavelet Transforms

1. Graps, Amara, Summer 1995, "An Introduction to Wavelets," *IEEE Computational Sciences and Engineering*, **2**, n.2, pp 50-61.

2. Strang, G., 1993, "Wavelet Transforms vs. Fourier Transforms," *Bulletin (New Series) of AMS*, **28**(2), pp. 288-305.

3. Mallat, S.G., 1989, "A theory for multiresolution signal decomposition: the wavelet representation," *IEEE Trans. PAMI*, **11**, 674-693.

4. Williams, John R., Amaratunga, Kevin, 1994, "Introduction to Wavelets in Engineering," *International Journal for Numerical Methods in Engineering*, **37**, 2365-2388.

5. Daubechies, I., 1992, *Ten Lectures on Wavelets*, SIAM, Philadelphia, PA.

6. Daubechies, I., 1988, "Orthonormal bases of compactly supported wavelets," *Commun. Pure Appl. Math.*, **41**, 909-996.

7. Vetterli, M. and Kovacevic, J., 1995, *Wavelets and Subband Coding*, Prentice Hall, Englewood Cliffs, NJ.